JOURNAL OF THERMOPHYSICS AND HEAT TRANSFER
Vol. 9, No. 1, January–March 1995

Influence of Exit Angle on Radial Jet Reattachment and Heat Transfer

H. Laschefski,* T. Cziesla,† and N. K. Mitra‡
Institut für Thermo- und Fluiddynamik, Ruhr-Universität Bochum, D-4630 Bochum, Germany

Flowfield and heat transfer have been computed for impinging laminar, semienclosed axial, and vectored radial jets. A finite volume computational scheme based on SIMPLEC has been developed to solve the Navier-Stokes and energy equations. The present scheme can handle backflow at the exit of the computational domain. The results show that the axial jets produce larger heat transfer on a small area, and the radial jets produce moderately large transfer on larger areas. Through the vectoring of the radial jets, the area of high transfer can be selected as wanted. Axial jets always give larger peak heat transfer on the point of impingement than the radial jet on the impingement circle. This peak value for radial jet increases with the increasing angle of the jet inclination. At some critical value of the jet inclination (60 deg for the present geometry and the Reynolds number) the total heat transfer on the impingement surface can be larger for the radial jet than for the axial jet. Radial jets with an angle of inclination of 0 deg or less can produce a suction force on the impingement surface. Such jets can be used for transport of the product surfaces and heat or mass transfer on the surface at the same time.

Nomenclature

a = temperature diffusivity
H = height of the confining wall
h = height of the jet from the impingement surface
L = radius of the impingement surface
Nu = Nusselt number
Pr = Prandtl number
p = pressure
R = radius of the feed tube
Re = Reynolds number
r = radial coordinate
T = temperature
t = time
u = axial velocity
v = radial velocity
x = axial coordinate
λ = thermal conductivity of the fluid
μ = kinematic viscosity
ν = dynamic viscosity
ρ = density

Subscripts
av = average value
in = inlet
w = impinging surface

Introduction

IMPINGING jets are used for heating, cooling, or drying of surfaces. They find applications in paper, glass or textile industries, and electronic cooling. These jets discharge from round or rectangular slots. They can be axial or radial (Figs. 1 and 2). At the point of impinging an axial jet produces large transfer rates, and away from the impinging point the transfer rate decreases rapidly.

A radial jet (Fig. 2) discharges from the side of the feed tube and reattaches on the impinging plate because of the Coanda effect. Here, instead of reattachment point, one obtains a reattachment line in form of a closed curve. The transfer coefficient is moderately high on the reattachment line and decreases away from it. For a round feed tube the radius of the reattachment circle depends on geometrical and flow parameters. The main advantage of a radial jet is that the moderately high heat or mass transfer can be distributed on a larger area than the axial jet; the size and the location of this area as well as the flux density can be easily controlled by changing the geometrical parameter (e.g., distance between the jet and the impinging plate h) or the flow parameters (e.g., the Reynolds number at the jet discharge). For an axial jet these parameters can essentially change the flux density at the reattachment point.

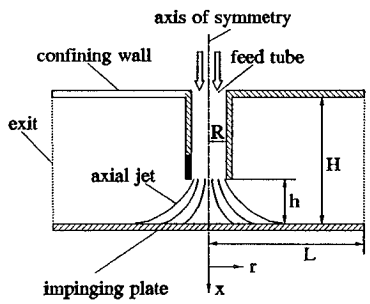

Fig. 1 Schematic of a semienclosed impinging axial jet.

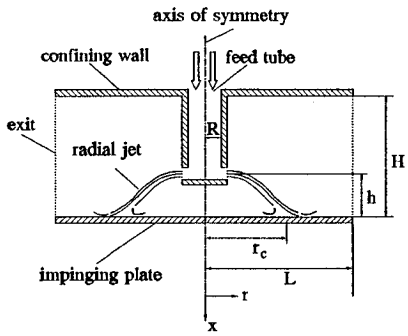

Fig. 2 Schematic of a semienclosed impinging radial jet.

Received May 7, 1993; revision received May 9, 1994; accepted for publication May 10, 1994.

*Scientific coworker, Postfach 102148.
†Student of Mechanical Engineering, Postfach 102148.
‡Professor, Postfach 102148. Member AIAA.

Although a large number of experimental studies of heat and mass transfer have been reported for impinging axial jets,[1,2] there have been limited studies concerning radial jets.

For laminar and turbulent radial jets with impinging plate, Page et al.[3] made an analytical study of the reattachment assuming that the velocity profile of the jet can be described by the boundary-layer theory. Their results predict reasonably well the reattachment radius of a turbulent jet, but they cannot predict near or far fields of the flow. Ostowari et al.[4] have presented experimental results of heat transfer on the impinging plate for turbulent radial jets.

Some preliminary results of numerical simulations of impinging axial and radial laminar jets from the solutions Navier-Stokes and energy equations have been reported by Laschefski et al.[5] These results show the complexity of the radial jet reattachment flowfield. The reattachment radius increases with the Reynolds number and the distance of the impingement plate. The reattachment stream surface covers the impingement plate like an umbrella. In the covered zone a separated flow characterized by a doughnut-shaped vortex ring appears. A flow reversal takes place at the nominal exit. Ambient fluid is sucked in the computational domain through part of the exit.[2,3] This makes the specification of the dynamic and thermal boundary conditions at the exit difficult and critical. The axial jets give extremely large heat transfer on a small area less than 5% of the impinging surface, whereas the radial jets give uniform and moderately high heat transfer on a large area (90% of the impingement surface).

The computations of Ref. 5 were done for a radial jet whose axis at the discharge was parallel to the impinging surface. Radial jets can be constructed in such ways that the jet axis at the discharge can have any arbitrary angle of inclination with respect to the impingement surface. If for the case of the jet axis at the discharge parallel to the surface the radial jet is said to have an angle of inclination of 0 deg, then the radial jet of angle of inclination of 90 deg becomes identical to an axial annular jet. With the angle of inclination the reattachment radius with high transfer rate can be controlled. Ostowari et al.[4] experimentally investigated the effect of the exit angle on the transfer rate of a turbulent radial jet. They measured heat transfer coefficient distribution for the angle of incidence $\vartheta = -10$, 0, 10, and 45 deg (Fig. 3a). They found the worst heat transfer with $\vartheta = -10$ deg, i.e., when jet is pointing upward and away from the reattachment plate and best heat transfer coefficients for $\vartheta = 45$ deg. It should be noted that the heat transfer is also strongly dependent on the distance between jet and the reattachment plate.[4,5] An optimum angle of inclination for any distance has not been obtained in Ref. 4.

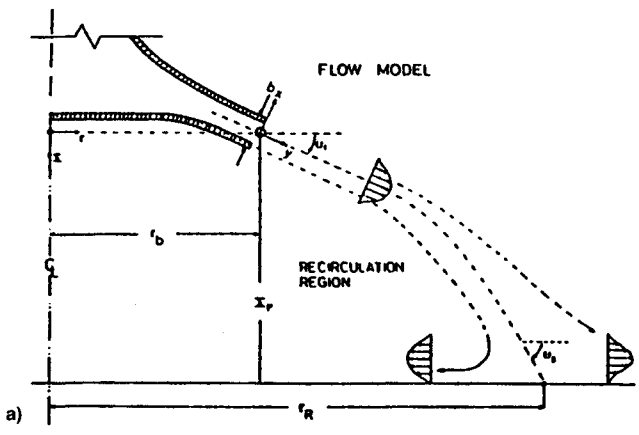

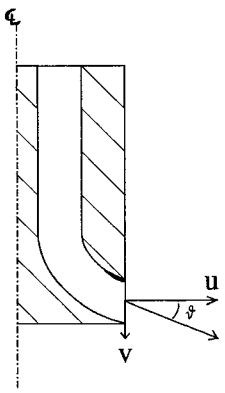

Fig. 3 Schematic of vectored radial jet with angle of inclination ϑ.[4]

The construction of the radial jet of Fig. 3a is such that the jet discharges normally to the exit plane. However, the jet apparatus can be constructed in a different way (Fig. 3b) so that the fluid comes out with an angle to the exit plane. The difference between Figs. 3a and 3b is the fact that for a given mass flow the momentum flux for the Fig. 3b will be larger than that for Fig. 3a. The computations of Ref. 5 show that the total heat transfer on a given area of the reattachment plate for a radial jet with $\vartheta = 0$ deg approaches that of the equivalent axial jet as the distance between the feed tube and the reattachment plate decreases. The influence of the angle of inclination, especially whether for some optimum angle of inclination the heat transfer for radial jet can be larger than an axial jet, is not known.

The purpose of the present work is the numerical simulation of radial reattaching jets on an impinging surface and the investigation of the effect of the angle of incidence on the transfer rate. The investigations are carried out by solving Navier-Stokes and energy equations. As radial jets with inclined angle of exit, only such geometry as in Fig. 3b is considered. In the present work only laminar jets are considered since in many applications, e.g., electronic cooling, such laminar jets may be encountered. The main difficulty in the turbulent flow computations is the selection of a proper turbulence model. Because of the large curvature effects, the standard models (e.g., k-ε model) are not reliable.[6] In the present work, the jet is semienclosed, i.e., a confining wall is placed on the top. This is again possibly typical in electronic applications. Finally, in order to identify the influence of the jet inclination alone, the effect of free convection has been neglected in the present work. Free convection will be of importance when the characteristic Grashof number is at least as large as the square of the characteristic Reynolds number. The important parameter for the Grashof number is the temperature difference of the impingement surface and the fluid or the heat flux on or from the impingement surface. The effect of the free convection will be reported in a future paper.

Basic Equations and Boundary Conditions

We consider only axisymmetric jets. The flowfield is described by the continuity, momentum (Navier-Stokes), and energy equations in cylindrical polar coordinates (Fig. 4a). The angle of inclination can be taken care of by vectoring the velocity profile at the jet discharge (Fig. 4b).

The basic equations written in nonsteady form for an incompressible fluid with constant properties are

Continuity equation

$$\frac{\partial(ur)}{\partial x} + \frac{\partial(vr)}{\partial r} = 0 \tag{1}$$

Axial momentum equation

$$\frac{\partial u}{\partial t} + u\frac{\partial u}{\partial x} + v\frac{\partial u}{\partial r} = -\frac{1}{\rho}\frac{\partial p}{\partial x} + \frac{\mu}{\rho}\nabla^2 u \tag{2}$$

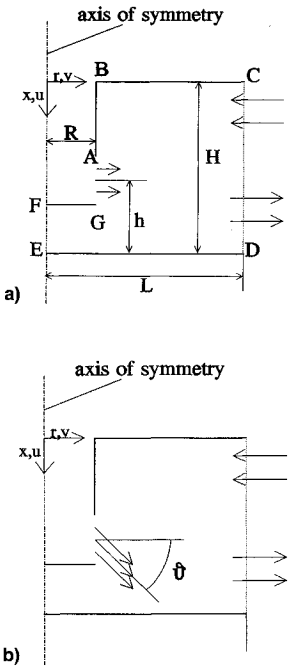

Fig. 4 a) Computational domain of a radial jet and b) schematic of the model of a vectored radial jet with the angle of inclination ϑ.

Radial momentum equation

$$\frac{\partial v}{\partial t} + u\frac{\partial v}{\partial x} + v\frac{\partial v}{\partial r} = -\frac{1}{\rho}\frac{\partial p}{\partial r} + \frac{\mu}{\rho}\nabla^2 v \tag{3}$$

Energy equation (neglecting the terms of dissipation)

$$\frac{\partial T}{\partial t} + u\frac{\partial T}{\partial x} + v\frac{\partial T}{\partial r} = a\nabla^2 T \tag{4}$$

The basic equations are nondimensionalized as $\bar{u} = u/u_{av}$, $\bar{v} = v/u_{av}$, $\bar{p} = (p - p_\infty)/(\rho u_{av}^2)$, $\bar{x} = x/R$, $\bar{r} = r/R$, $\bar{L} = L/R$, $\bar{h} = h/R$, $\bar{H} = H/R$. Here, u_{av} is the average velocity at the exit, and p_∞ is the reference (atmospheric) pressure. The temperature is nondimensionalized as $\bar{T} = T/T_{in}$.

The dimensionless equations contain as parameters the Reynolds number $Re = u_{av}R/\nu$ and the Prandtl number $Pr = \nu/a$. The nondimensional equations will not be presented here.

The assumptions of constant properties and negligible dissipation requires small temperature difference and velocity (or *Ma* number) of the flow. In many industrial cooling systems, the second assumption is quite justified. The first one was made in order to reduce the computational effort. No-slip conditions are used on the solid walls:

$$u = v = 0 \tag{5}$$

At the jet discharge measured or physically feasible velocity profiles for u and v can be used. The main problem is the specification of the nominal outflow boundary conditions at CD (Fig. 4a), since this boundary condition should allow that the ambient fluid is sucked into the computational domain across the upper part of the boundary, and the fluid leaves the computational domain across the lower part of CD. It should be mentioned that the radius of the computational domain L is chosen arbitrarily.

The computational results should be reasonably independent of the value of L or the position of CD. This problem of the outflow boundary condition has been discussed by Rannacher,[7] who suggested a "natural" condition, which in dimensionless form is given by

$$\partial_n v + p = 0 \tag{6}$$

where ∂_n stands for the gradient of the velocity vector v in the normal direction to the boundary. Equation (6) implies that for a constant exit pressure, the velocity gradient in the normal direction at the exit plane is zero. Computational tests of flowfields in a channel with an obstacle (von Kármán vortex street) show that the boundary condition Eq. (6) is independent of the length of the computational domain.[7] Such tests have also been performed in the present work. The "hidden" boundary condition for the pressure is discussed in the next section.

The impingement plate is isothermal with a temperature T_w, which is different from T_{in}, the jet temperature at discharge. The ambient air is also assumed to have a temperature T_{in}. The solid surfaces besides the impingement plate are assumed to be adiabatic. The thermal condition at the nominal exit CD is made dependent on the velocity. If the fluid leaves the computational domain, the radial gradient of the temperature is set equal to zero. If the fluid enters the computational domain from the ambient, the Dirichlet condition with T_{in} is used. In the following computations nondimensional T_{in} is set equal to 1, and $T_w = 1.05$.

Method of Solution

The continuity and the momentum equations are solved by a modified SIMPLE[8]-based, time-dependent finite volume technique on colocated grids. The flowfield in this scheme is obtained in two steps. In the first step the momentum equations are solved for a known pressure field. In the second step the solution of the continuity equation is obtained by a pressure-velocity correction in each discrete cell until a locally solenoidal velocity field is obtained.

The pressure-velocity correction of original SIMPLE[9] or SIMPLEC[8] fails to converge for the present problem. A close examination showed that the hidden boundary condition for the pressure at the exit CD is the normal gradient of the pressure correction term:

$$\frac{\partial p'}{\partial n} = 0 \tag{7}$$

This does not allow pressure or velocity correction at CD. In the original SIMPLE the velocity at CD is corrected in such a way that the global mass flow rate is satisfied. However, with backflow at CD the global mass flow is not a priori known.

In the present work the hidden pressure boundary condition at CD is modified, and instead of Eq. (6), constant pressure at CD is used. This along with some extrapolations from the interior points allows velocity correction on CD without imposing the global continuity. The details can be seen in Ref. 10.

In the present computations parabolic profiles at the jet discharge have been assumed. For the radial jet the height of the opening (AG in Fig. 4a) is taken as equal to R so that the mass flow and the average velocity at the discharge of the axial and radial jets are always the same.

Results and Discussion

A large number of computations have been performed with angles of inclination $\vartheta = -10$–80 deg, with increments of 10 deg. For all these cases the characteristic Reynolds number is kept fixed at 2.5×10^2. The nondimensional height of the jet axis from the impingement plate is 2, and the height of the confining wall is 5. The nondimensional radius of the impingement plate is chosen to be 10. These geometrical parameters are chosen because some detailed computational results for the axial jets have been carried out previously.[5,10] In all the cases steady flows have been obtained. Nonsteady or turbulent flows result at higher Reynolds numbers.[10]

Computations have been carried out on (102 × 202) grids on an IBM 600/530H workstation. Studies with finer grids

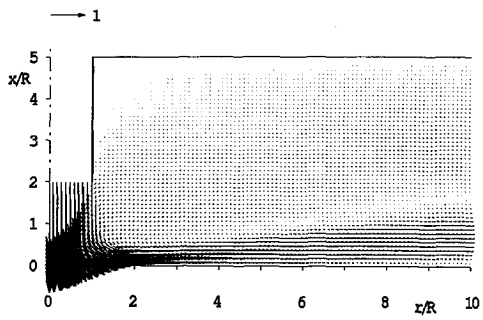

Fig. 5 Velocity vectors of a steady axial jet, $Re = 2.5 \times 10^2$.

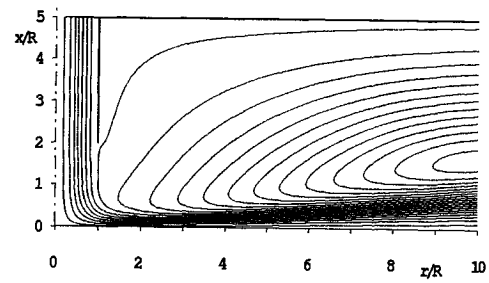

Fig. 6 Streamlines of an impinging axial jet, $Re = 2.5 \times 10^2$.

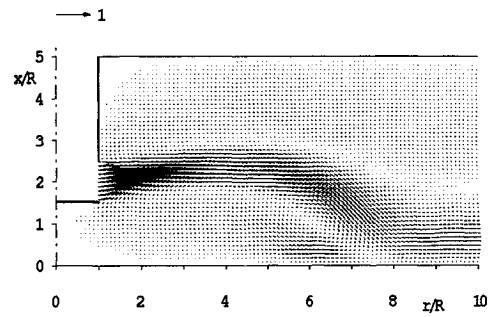

Fig. 7 Velocity vectors of a steading impinging radial jet. Angle of inclination $\vartheta = -10$, $Re = 2.5 \times 10^2$.

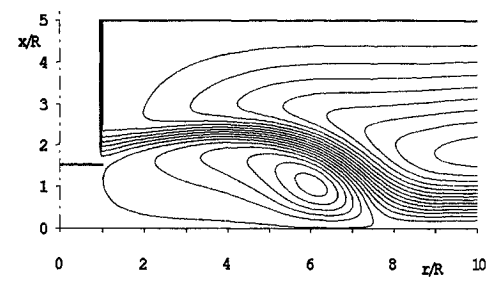

Fig. 8 Streamlines of a steading impinging radial jet. Angle of inclination $\vartheta = -10$, $Re = 2.5 \times 10^2$.

(202 × 402) showed that average Nusselt number obtained with the present grid differed from the grid-independent Nusselt number by less than 3%. Figure 5 shows the velocity vectors of the axial jet. The jet after impinging develops like a wall jet on the impingement surface. Ambient fluid moves in through the upper part of the exit. This is quite clear from the streamlines shown in Fig. 6. Figures 7 and 8 show the velocity vectors and the streamlines for the radial jet with $\vartheta = -10$ deg. Corresponding flow streamlines for $\vartheta = 0$, 20, and 70 deg are shown in Figs. 9, 10, and 11, respectively. For $\vartheta = -10$ deg, the jet is directed upwards at the exit,

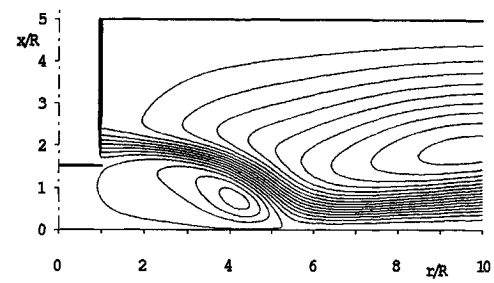

Fig. 9 Streamlines of a steading impinging radial jet. Angle of inclination $\vartheta = 0$ deg, $Re = 2.5 \times 10^2$.

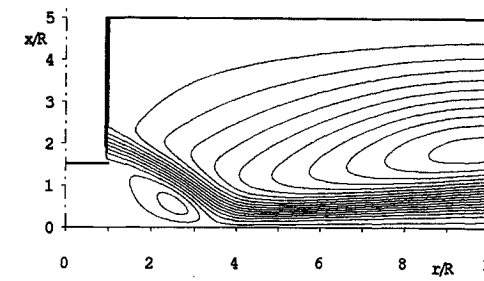

Fig. 10 Streamlines of a steading impinging radial jet. Angle of inclination $\vartheta = -20$ deg, $Re = 2.5 \times 10^2$.

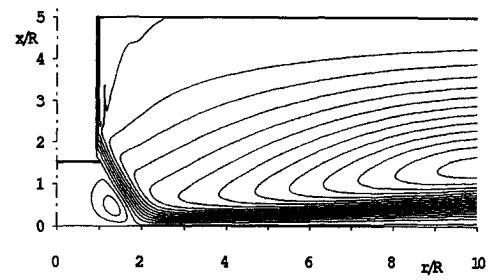

Fig. 11 Streamlines of a steading impinging radial jet. Angle of inclination $\vartheta = -70$ deg, $Re = 2.5 \times 10^2$.

then it bends downwards due to a Coanda effect, and reattaches at $r/R = 7.5$. Between $r/R = 0$ and the reattachment line a separated zone with a vortex ring with center at $r/R = 6$ appears. This is also clearly seen in Fig. 8.

With increasing ϑ the reattachment radius becomes smaller. For $\vartheta = 0$ deg, the nondimensional reattachment radius is 5.2. The corresponding values for $\vartheta = 20$ deg is 3.3, and for $\vartheta = 70$ deg it is 1.9. The center of the ring vortex also moves towards the center of the plate as ϑ increases (Figs. 9–11). The vortex core also becomes slimmer as ϑ increases. Otherwise the flow structure remains qualitatively the same for all values of ϑ.

Figure 12 compares the local Nusselt number distribution on the impingement plate. The Nusselt number is defined as

$$Nu(r) = \frac{\dot{q}R}{\lambda(T_w - T_{in})}$$

where $\dot{q}$ is the local heat flux on the impingement surface. $Nu(r)$ then represents the nondimensional heat flux on the impingement plate.

Table 1 compares the area-averaged Nusselt numbers, locations of the maximum local Nusselt numbers, locations of the reattachment, and the nondimensional pressure force on the impingement plate. The nondimensional pressure force is calculated as

$$\int_0^{\bar{L}} \bar{p}\bar{r}\, d\bar{r}$$

Table 1 Comparison Nusselt number and nondimensional force on the impingement surface

Angle of inclination	Average *Nu*	Location of maximum *Nu*	Reattachment point	Nondimensional force
Axial jet	2.18	0	0	4.225
Radial jet, deg				
−10	1.31	7.475	7.6	−0.521
0	1.52	5.274	5.3	−0.09
10	1.60	4.175	4.15	0.245
20	1.68	3.475	3.4	0.607
30	1.77	2.975	2.9	1.031
40	1.88	2.575	2.55	1.563
50	2.03	2.325	2.25	2.295
60	2.22	2.075	2.05	3.443
70	2.52	1.875	1.85	5.671
80	3.16	1.675	1.65	12.665

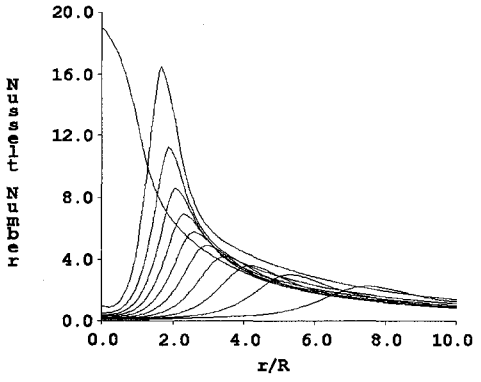

Fig. 12 Local Nusselt number distribution on the impingement surface for the axial and radial jets. The angle of inclination of the radial jet is varied from the 80 to −10 deg, at 10-deg intervals. The curve with highest peak corresponds to 80 deg, and the lowest peak to −10 deg. The intermediate peaks correspond to intermediate angles, $Re = 2.5 \times 10^2$.

The location of the reattachment point has been obtained from the local friction factor distribution. The pressure force has been obtained by integrating the difference between local pressure and the atmospheric pressure on the impingement surface. Figure 12 shows, as expected, that the axial jet has a peak in *Nu* at the center, i.e., at the impingement point. This peak value is 19. Away from the center, *Nu* falls down very fast and becomes less than its average value of 2.18 at $r/R = 5$. For the radial jet, the peak in *Nu* appears close to the reattachment point. Hence, the peaks show a shift towards the right, depending on the inclination angle.

For radial jet with $\vartheta = -10$ deg, the *Nu* is extremely small at the separated dead water zone in the center of the impingement plate. *Nu* increases slowly at first, then steeply to a peak of 2.3, slightly ahead of the reattachment circle. After that it falls down. This behavior is qualitatively repeated for all angles of inclination. However, the peak value of *Nu* increases with ϑ and its location, which is the center. The increase in the peak *Nu* is not linearly dependent on the angle, but increases with the angle of inclination. It should also be mentioned that the peak *Nu* for the axial jet is still nearly 20% larger than the highest peak of 16 for the radial jet for $\vartheta = 80$ deg. However, the decrease in the *Nu* away from the peak for the radial jets is slower than that of the axial jet. This suggests that the average Nusselt number for the radial jets may show more impressive performance than the local *Nu*. Table 1 shows that at $\vartheta = 60$ deg, $\overline{Nu}$ for the radial jet becomes nearly the same as that for the axial jet. With $\vartheta = 80$ deg, the heat transfer for the radial jet can be 50% larger than for the axial jet. It should be noted here that the average value of the Nusselt number (i.e., the average heat transfer) depends on the size (i.e., the radius) of the impingement plate. The present size $r/R = 10$ has been chosen arbitrarily. For an even larger impingement surface the radial jet will be more advantageous than the axial jet because of the steep decrease in the Nusselt number for the axial jet.

Table 1 also shows that maximum *Nu* appears slightly before the reattachment point for $\vartheta = -10$ and 0 deg, and slightly after the reattachment point for $\vartheta > 0$ deg. This behavior has also been observed in experiments.[3] It is also interesting to note that for $\vartheta \leq 0$ deg, the total pressure force on the impingement plate is negative, i.e., the impingement surface feels a suction force towards the jet. This has also been observed in experiments and has found application in industries. The pressure force for an 80-deg jet is much larger than that for the axial jet because the pressure force is much larger because of the larger momentum flux.

Conclusions

Numerical simulation of semienclosed impinging axial and radial laminar jets show that the peak heat transfer for an axial jet at the reattachment point is always larger than the peak heat transfer at the reattachment circle for the radial jet. However, for the axial jet, the heat transfer reduces quickly away from the reattachment point, whereas for the radial jet, moderately high transfer rate can be obtained on a much larger area than the axial jet. If the radial jet is vectored, the location of the high transfer rate can be changed. The total heat transfer on the impinging plate can be larger for the radial jets with a 60-deg or more angle of inclination than for the axial jet. As the inclination angle is reduced, the total heat transfer can decrease very much in comparison to the axial jet. The radial jet with angle of inclination of 0 deg or less exerts a suction force on the impingement plate. This characteristic can be used for transport, heating, cooling, or drying of product surfaces at the same time.

Acknowledgments

This work has been supported by the Deutsche Forschungsgemeinschaft. The authors would like to thank R. H. Page of Texas A&M University, College Station, Texas, for suggesting this problem and many helpful discussions.

References

[1]Martin, H., "Heat and Mass Transfer Between Impinging Gas Jets and Solid Surfaces," *Advances in Heat Transfer*, Vol. 13, Academic Press, New York, 1977, pp. 1–60.

[2]Viskanta, R., "Heat Transfer to Impinging Isothermal Gas and Flame Jets," *Experimental Thermal and Fluid Science*, Vol. 6, No. 2, 1993, pp. 111–134.

[3]Page, R. H., Hadden, L. L., and Ostowari, C., "Theory for Radial Jet Reattachment Flow," *AIAA Journal*, Vol. 27, No. 11, 1989, pp. 1500–1505.

[4]Ostowari, C., Paikert, B., and Page, R. H., "Heat Transfer Measurement of Radial Jet Reattachment on a Flat Plate," National Fluid Dynamics Congress, Cincinnati, OH, July 1988.

[5]Laschefski, H., Holl, A., Grosse-Gorgemann, A., Mitra, N. K., and Page, R. H., "Flow Structure and Heat Transfer of Radial and Axial Jet Reattachment on a Flat Plate," American Society of Me-

chanical Engineers, ASME HTD-Vol. 210, 1992.

[6]Yap, C. R., "Turbulent Heat and Momentum Transfer in Recirculating and Impinging Flows," Ph.D. Dissertation, Victoria Univ. of Manchester, Manchester, England, UK, 1987.

[7]Rannacher, R., "On the Numerical Solution of Incompressible Navier-Stokes Equations," *Zeitschrift für Angewandte Mathematik und Mechanik*, Vol. 73, No. 9, 1993, pp. 203–216.

[8]Doormaal, Van, J. P., and Raithby, G. D., "Enhancement of the SIMPLE Method for Predicting Incompressible Fluid Flows," *Numerical Heat Transfer*, Vol. 7, No. 2, 1984, pp. 147–163.

[9]Patankar, S. V., *Numerical Heat Transfer and Fluid Flow*, Hemisphere, Washington, DC, 1980.

[10]Laschefski, H., Braess, D., and Mitra, N. K., "Numerical Investigation of Radial Jet Reattachment Flows," *International Journal for Numerical Methods in Fluids*, Vol. 18, No. 7, 1994, pp. 629–646.

[11]Page, R. H., private communication, Texas A&M Univ., Dept. of Mechanical Engineering, College Station, TX.